

# CHARACTERIZATION OF POROUS GRAPHITE AIR BEARINGS

Byron R. Knapp, Brian P. O'Connor, Eric R. Marsh  
Machine Dynamics Research Lab  
The Pennsylvania State University, University Park, PA

## Introduction

As the demand for higher precision machine tools and inspection equipment grows, there is a need for more precise bearing systems. The error motions of bearings with mechanical contact are dominated by the geometric and surface finish errors of their components [1]. Air bearings, however, do not have mechanical contact between elements and benefit from an air-film averaging effect. Furthermore, due to an absence of mechanical contact, the air bearing has virtually no friction to generate heat and cause wear.

An ideal air bearing would distribute the pressure equally across the entire bearing face to increase load capacity and stiffness. By using bearings with porous media compensation, the pressure distribution is nearly constant across the entire face of the air bearing. In addition to their inherent high stiffness and load carrying capacity, porous media air bearings offer better damping and stability characteristics compared to orifice compensated designs [2, 3].

A substantial amount of work has been done to improve the quality of porous graphite air bearings since the work published by Rasnick et al. [2]. The objective of this research is to develop an empirical stiffness model for porous graphite air bearings and verify this model using experimental modal and finite element analyses. The importance of establishing a model for structural performance is evident with respect to deterministic design.

## Experimental Approach

Static load tests are performed on New Way Machine Components porous graphite air bearing pads. A 3-axis Kistler load cell is used to measure the applied force to the air pad. Lion Precision capacitance probes are mounted directly to the back of the air pad to measure the air-film thickness. The bearing pads are tested at supply pressures ranging from 350 kPa (50 psi) to 690 kPa (100 psi) in order to investigate the effect of supply pressure and air-film thickness on pad stiffness. An example of the load versus air-film displacement data is shown in Figure 1.

Load versus air-film displacement data from each static load test is curve fit to a polynomial. The experimental stiffness ( $K_{Static}$ ) values are obtained by evaluating the derivative of the curve at specific air-film thicknesses. By normalizing the static stiffness by the supply pressure ( $P$ ), air-film thickness ( $G$ ), and effective bearing area ( $A$ ), a constant stiffness factor ( $C_k$ ) is found using Equation 1.

$$C_k \approx \frac{K_{Static}}{\left(\frac{A \cdot P}{G}\right)} \quad (1)$$

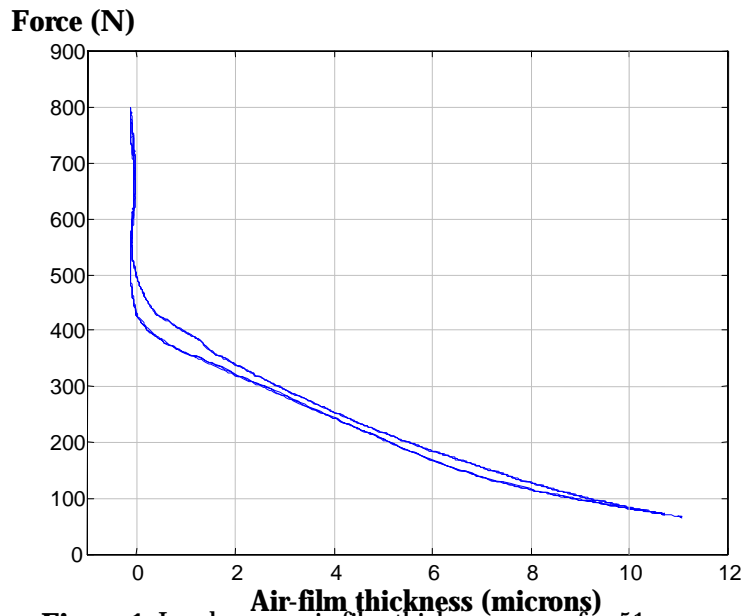


**Figure 1:** Load versus air-film thickness curve for 51 mm pad at 380 kPa supply.

The stiffness factor,  $C_k$ , shown graphically in Figure 2, is found by curve fitting a line to the normalized data. The slope of the line,  $C_k$ , is 0.26. The  $R^2$  value for the regression is 0.95, meaning that the linear model is a very good approximation of the data.

It is interesting to note that Rasnick of Oak Ridge Y-12 used a similar method for approximating the stiffness [4]. He quotes a stiffness factor of 0.35 for a captured thrust porous graphite air bearing.

The static stiffness ( $K_{Static}$ ) of the porous graphite air pad is calculated for air-film thicknesses greater than 3 microns as

$$K_{Static} = 0.26 \left( \frac{A \cdot P}{G} \right) \quad (2)$$

For air-film thicknesses less than 3 microns, the stiffness does not change proportionally with  $A$ ,  $P$ , and  $G$ . Therefore, Equation 2 cannot be applied for air-film thicknesses less than 3 microns.

Using static load tests to find the stiffness of a simple porous graphite air bearing pad has been shown a straightforward process. This same technique can be used to determine the stiffness characteristics of more complicated bearing systems as well. However, a more elegant approach is to determine the static stiffness using Experimental Modal Analysis (EMA). To determine the stiffness of the bearing using EMA, the modal mass and resonance must be determined. For a simple spring-mass oscillator, the stiffness is determined given the mass and natural frequency. Unfortunately, most bearing systems do not follow this simple model since the dynamics of the structure and the air layer become coupled.

To find the static stiffness of a New Way air bearing stage (box slide with four air pads and solid aluminum ram, shown in Figure 3), a modal analysis is conducted. The results of the experimental analysis are summarized in Table 1. The first six natural modes are below 2500 Hz; the first three modes reflect air layer dynamics, while the second three are predominately structural. Since the pitch, roll, and bounce modes involve compression of the air layer, they are the most influential in determining the air layer stiffness.

**Table 1:** Experimental modal results.

MODE	Frequency (Hz)	Damping (%)	DESCRIPTION OF MODE
1	870	5.0 %	Pitch
2	1020	5.9 %	Roll
3	1250	1.4 %	Bounce
4	1610	1.6 %	Box slide shear
5	1880	0.8 %	Box slide torsion
6	2230	1.5 %	Ram and slide bending

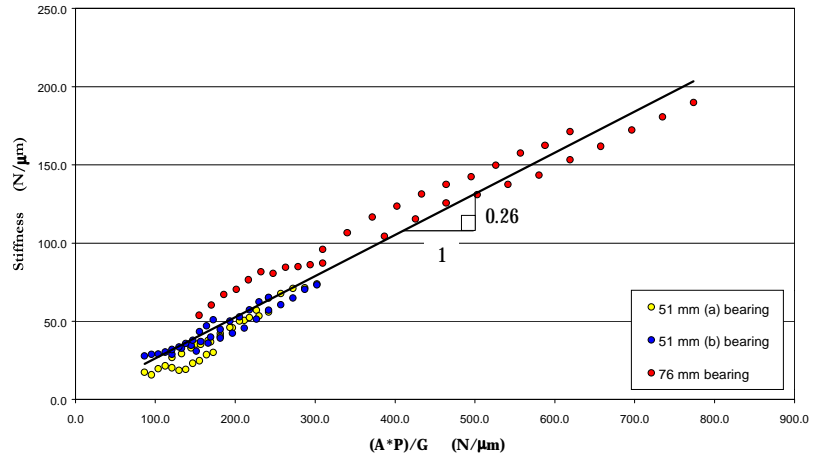


**Figure 2:** Porous graphite stiffness factor for 4, 5, 7, and 10 micron air-film thicknesses.

A finite element model of the linear air stage is developed using FEA software. The air stage, shown in Figure 3, is modeled in three parts: 1) ram and box slide – modeled as solid aluminum components; 2) porous graphite – modeled as aluminum with an 80% lower modulus of elasticity; 3) air layer –

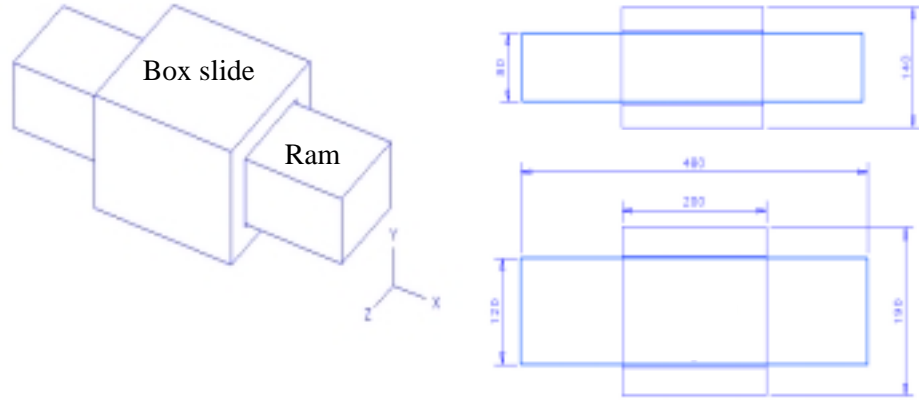


**Figure 3:** Finite element model of the air stage (dimensions in mm).

modeled as a 5x5 grid of discrete springs at each porous graphite-ram interface. J.M. Pitarresi uses a similar air layer finite element modeling technique (discrete springs) for the calculation of the dynamic stiffness of an air bearing pad [5]. In order to determine the variation of the stiffness of the air layer due to internal air pressure, a static analysis of a  $1/8$  model of the box slide is conducted. The deflection of the box ranges from 6 to 12 microns under normal operating conditions, which results in a significant variation in the air layer stiffness. Therefore, the stiffness along the  $Y$  face is varied from  $k_y$  at the corner to  $k_y/2$  at the center (based on the static stiffness model of Equation 2). The stiffness along the  $Z$  face is kept constant at  $k_z = 0.6 k_y$  because while the gap remains constant in that direction, the area is 60% of the area along the  $Y$  face.

The air gap stiffness is determined by matching the experimental and finite element results. The stiffness of the discrete springs is varied until the first six frequencies of vibration match the experimental results. The stiffness in the  $Y$  direction is obtained by summing the discrete springs used to represent the air-layer. Unfortunately, due to inaccurate modeling (such as modeling the box slide as one solid piece, unmodeled damping, etc.), each individual mode converges to the experimental data at a slightly different air-layer stiffness. The air-layer stiffness which corresponds to the least amount of error,  $K_y = 560$  N/micron, can be found in Table 2.

**Table 2:** Percent error in model updating.

Stiffness (N/ $\mu$ m)		% Error Between Experimental and Finite Element Analyses						RMS
$K_y$	$K_z$	Pitch	Roll	Bounce	Shear	Torsion	Bending	Error
385	482	-6	-13	-30	14	1	-14	6.5
403	503	-4	-12	-29	14	1	-13	6.2
420	525	-2	-10	-28	15	1	-13	6.0
438	547	-1	-9	-28	15	1	-12	5.8
455	569	1	-7	-27	15	2	-12	5.7
490	613	4	-5	-26	16	2	-11	5.4
525	657	6	-2	-25	16	2	-9	5.3
560	700	9	0	-23	17	3	-8	5.2
595	744	11	2	-23	17	3	-7	5.3
630	788	13	4	-22	18	3	-6	5.4
700	876	17	8	-20	19	4	-4	5.7

Using the results obtained from the FEA and the EMA, the static stiffness model of Equation 2 is verified. The air stage was tested at a supply pressure of 410 kPa. Since the static FEA of the box slide shows that the air-film thickness varies from 6 to 12 microns over the top face of the air stage, an average air-film gap of 9 microns is used. The air stage has two opposing pads; consequently the stiffness is doubled.

$$K_{Static} = C_k \frac{PA}{G} = 0.26 \frac{(410 \text{ kPa})(2)(120 \text{ mm})(200 \text{ mm})}{9 \mu\text{m}} = 570 \text{ N/micron}$$

## Conclusion

The calculated stiffness of 570 N/micron agrees within 5% of the stiffness predicted from the FEA analysis (560 N/micron). Thus, the static stiffness model developed proves to be very accurate in estimating the stiffness of the more complex linear air stage.

The results of this study advance the state of the art in precision machining and inspection through the development of design and measurement techniques for porous graphite air bearings. In addition, a method for finite element modeling of the stiffness of air-films in porous graphite air bearings is proposed.

## Acknowledgements

This research was made possible through funding provided by Tropel Corporation, New Way Machine Components, the National Science Foundation, Kistler Instrument Corporation, and Lion Precision. In addition, the authors are grateful for the many hours of discussion, consulting, and testing contributed by David A. Arneson and Melvin J. Liebers from Professional Instruments Company and fellow MDRL graduate student Robert D. Grejda.

## References

- [1] Slocum, A.H. *Precision Machine Design*. Dearborn, Michigan: Society of Manufacturing Engineers, 1992.
- [2] Sheinberg, S. A., and Shuster, V.G., *Machine and Tooling* v 31, 1960, p 24-29.
- [3] Sneck, H.J., "A Survey of Gas-Lubricated Porous Bearings." *Journal of Lubrication Technology*, October 1968, pp.804-809.
- [4] Rasnick, W.H., Steger, P.J., Arehart, T.A., and Littleton, D.E. "Porous Graphite Air Bearing Components as Applied to Machine Tools," *SME Technical Report MRR74-02*, 1974.
- [5] Pitarresi, J.M., and Haller, K.A. "An Air Layer Modeling Approach for Air and Air/Vacuum Bearings." *Journal of Manufacturing Science and Engineering* v 119, August 1997, pp. 388-392.

## Keywords

Porous Graphite Air Bearings, Modal Analysis, Finite Element Analysis